THE JOURNAL OF PHYSICAL CHEMISTRY Letters

pubs.acs.org/JPCL Letter

Structural Distortion and Bandgap Increase of Two-Dimensional Perovskites Induced by Trifluoromethyl Substitution on Spacer Cations

Pei-Xi Wang, Amin Morteza Najarian, Zhaomin Hao, Andrew Johnston, Oleksandr Voznyy, Sjoerd Hoogland, and Edward H. Sargent*

Cite This: *J. Phys. Chem. Lett.* 2020, 11, 10144−10149 Read Online

ACCESS | Metrics & More | Article Recommendations | Supporting Information

ABSTRACT: In further advancing display technologies, especially for improved blue emitters, to engineer the bandgap of promising semiconductors such as hybrid perovskites is important. Present-day methods for tuning the bandgaps of perovskites, such as the incorporation of mixed halide anions, suffer drawbacks such as phase separation and difficulty in synthesis. Here we report a new 2D lead iodide perovskite that emits in the blue spectral region. We exploit an increased angular distortion of PbI_4^{2-} octahedra to widen the bandgap of 2D metal halide perovskites. We synthesized 2D lead iodide perovskites based on $(4\text{-Y-}C_6H_4CH_2NH_3)_2PbI_4$ (Y = H, F, Cl, Br, I) and substituted the halogen atoms with a $-CF_3$ group to create $(4\text{-}CF_3\text{-}C_6H_4CH_2NH_3)_2PbI_4$ compounds. We observed that the CF_3-substituted material exhibited a ∼0.16 eV larger bandgap than did the halogen-substituted materials. We used X-ray diffraction and density functional theory simulations and found that the blue shift can be assigned to the angular distortion of the PbI_4^{2-} lattice, a distortion traceable to repulsive intermolecular interactions between the trifluoromethyl groups on oppositely-arranged spacers. These results add a degree of freedom in tuning 2D perovskites to selected bandgaps for optoelectronic applications.

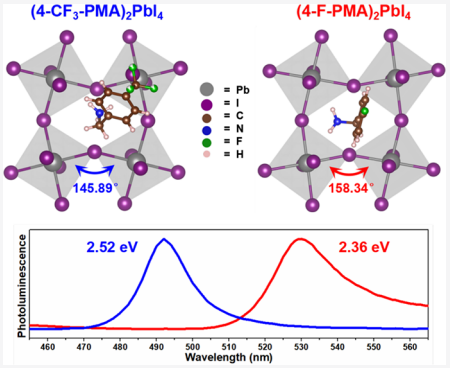

Organic−inorganic hybrid metal−halide perovskites have attracted scientific and technological interest in the past decade.[1,2] Two-dimensional (2D) metal−halide perovskites, in which the inorganic framework is separated by bulky organic spacers, have gained recent interest due to their promising stability, high photoluminescence quantum yield (PLQY), and narrow emission line widths.

In these materials, the negatively-charged metal−halide octahedra are arranged into parallel planes fully separated by cationic organic molecules.[3] The bandgap and therefore the optical and electronic properties of 2D tin and lead iodide perovskites can be modified by adjusting the angular distortion between adjacent metal−halide octahedra.[4−10] The bandgap of 2D perovskites increases as the metal−halide−metal bond angle deviates from the ideal value of 180°. For perovskites consisting of organic ammonium (R-NH_3) spacer cations, this angular distortion is attributed to the penetration of cationic $-NH_3^+$ groups below the planes of axial halogen atoms,[11] determined by intermolecular interactions among the organic −R moieties.

To evaluate the extent to which the bandgap of 2D perovskites can be enlarged by structural distortion, we reviewed the relationships between the photoluminescence (PL) emission wavelength and crystal structure in 2D lead iodide perovskites having different organic spacer cations (Table 1). In the case of spacers made up of unsubstituted, and *para*-halogen/methyl-substituted, phenylmethylammonium (4-Y-$C_6H_4CH_2NH_3$ where Y is the substituent group, abbreviated *Y*-PMA) and 2-phenylethylammonium (4-Y-$C_6H_4CH_2CH_2NH_3$, abbreviated as Y-PEA), the corresponding 2D perovskites $(\text{Y-PMA})_2PbI_4$ (Y = H, F, Cl, Br, I) and $(\text{Y-PEA})_2PbI_4$ (Y = H, F, Cl, Br, CH_3) exhibit similar PL bandgaps in the range 2.32−2.37 eV, where the Pb−I−Pb bond angle varies from 158.4° to 151.4° and the interlayer spacing distance ranges from 13.66 to 17.08 Å.[10,12]

We conclude that when aromatic spacers are used, creating additional separation among the inorganic layers through the use of longer organic moieties does not increase bandgap. Moreover, the much shorter halogen-terminated two-carbon aliphatic spacers $Y-(CH_2)_2-NH_3$ (Y = Cl, Br, I) do show a significantly enlarged bandgap (∼2.46 eV) along with a decreased Pb−I−Pb bond angle of 147.4°; the distortion was

Received: September 22, 2020
Accepted: November 9, 2020

https://dx.doi.org/10.1021/acs.jpclett.0c02909
J. Phys. Chem. Lett. 2020, 11, 10144−10149

Table 1. Comparison of Selected Structural and Optical Properties between $(CF_3\text{-PMA})_2PbI_4$ and 2D Lead Iodide Perovskites A_2PbI_4 with Other Organic Spacer Cations (Different "A" Moieties)

spacer cation A	PL bandgap (eV)	Pb−I−Pb angle (deg)	intralayer Pb−Pb distance (Å)	interlayer spacing (Å)
$Br-(CH_2)_2-NH_3$	2.25	176.92, 177.55	6.4824, 6.4583	10.5702
$Cl-(CH_2)_2-NH_3$	2.28	176.68, 178.07	6.4312, 6.4703	10.3982
H−PMA	2.32	157.52	6.2760	14.2039
I−PMA	2.32	156.11	6.2079	16.5128
F−PMA	2.36	158.00, 158.69	6.3105, 6.3812	13.6635
Cl−PMA	2.36	153.91, 155.07	6.1924, 6.2448	15.7889
Br−PMA	2.36	151.34, 154.75	6.1408, 6.2485	15.8030
H−PEA	2.37	151.44, 152.90	6.1121, 6.1715	16.0831
F−PEA	2.37	151.41	6.1185	16.3159
Cl−PEA	2.37	152.48	6.1389	16.6400
Br−PEA	2.37	152.15	6.1250	17.0645
CH_3-PEA	2.37	152.00, 152.42	6.1143, 6.1306	17.0803
$I-(CH_2)_2-NH_3$	2.46	147.38	6.1873	12.6072
CF_3-PMA	2.52	145.89	6.0496	17.9252

shown to be caused by iodine−iodine halogen bonding between the $I-(CH_2)_2-NH_3$ spacers and perovskite octahedra.[13] These results hinted that, if we could decrease the Pb−I−Pb angle to below 145°, this could further widen the bandgap of 2D perovskites.

To understand why the Y-PMA and Y-PEA spacers do not lead to a significantly distorted lattice, we investigated the crystal structures of $(Y\text{-PMA})_2PbI_4$ and $(Y\text{-PEA})_2PbI_4$. The attractive $\pi-\pi$ and π-halogen interactions between adjacent aromatic rings of these spacers compensate for the intermolecular steric hindrance repulsion.[12,14] We hypothesized that if we adopted instead a synthetic approach focused on increasing steric hindrance, and if we deployed functional groups that increase repulsive intermolecular interactions, we would have the opportunity to increase the bandgap of 2D perovskites. Trifluoromethyl groups ($-CF_3$) could facilitate this since there is a large electrostatic repulsion between $-CF_3$ groups or between $-CF_3$ groups and aromatic rings.[15] This repulsion is the result of high electron density around trifluoromethyl groups originating from the strong electronegativity of fluorine atoms.[16−19]

On the basis of the above hypothesis, we selected CF_3-PMA cations as organic spacers, with which we synthesized the 2D lead iodide perovskite, $(CF_3\text{-PMA})_2PbI_4$. We investigated the optoelectronic and crystallographic properties of the new perovskite and found it had a highly distorted crystal structure (Pb−I−Pb angle of 145.9°) and a significantly blue-shifted emission compared to its *para*-halogen-substituted analogues (Table 1, 2.52 eV versus ∼2.36 eV).

We synthesized $(CF_3\text{-PMA})_2PbI_4$ 2D perovskites using a slow cooling crystallization method. A hot (373 K) aqueous solution containing hydroiodic acid (6.30 mol/L), hypophosphorous acid (1.50 mol/L), lead iodide (0.15 mol/L), and 4-

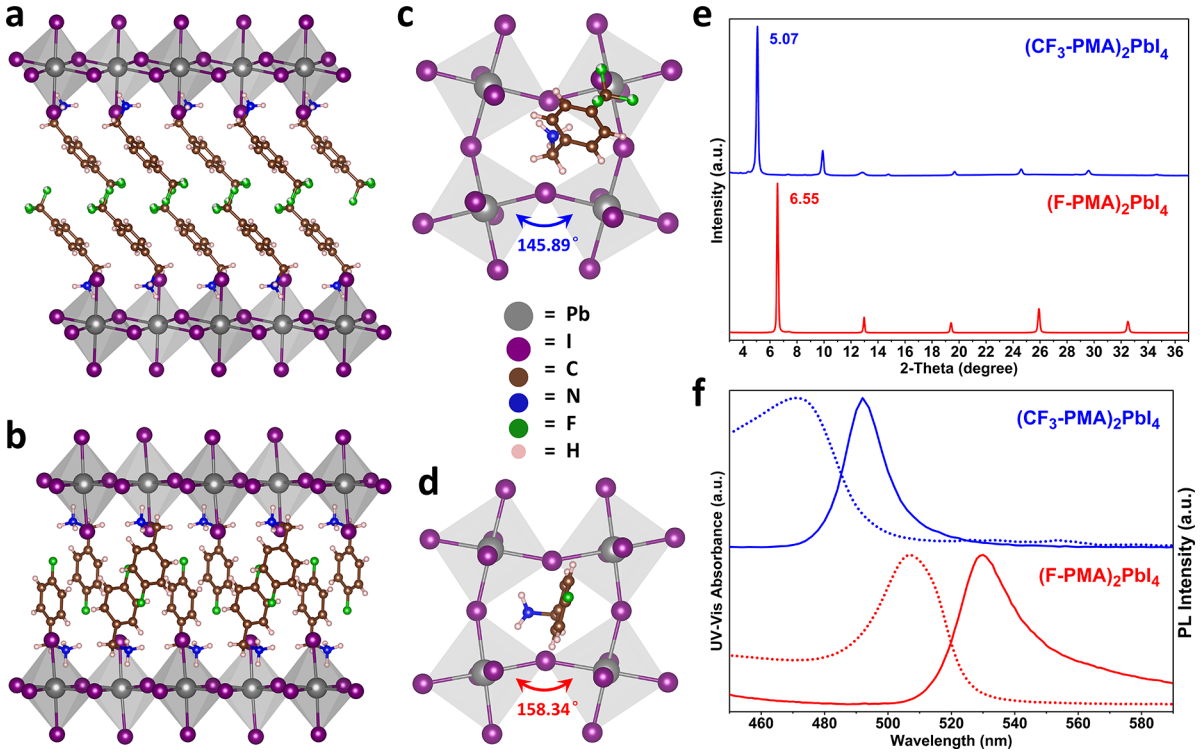

Figure 1. (a)−(d) Crystal structures obtained with single-crystal X-ray diffraction of $(CF_3\text{-PMA})_2PbI_4$ (a, c) and $(F\text{-PMA})_2PbI_4$ (b, d) viewed from directions parallel (a, b) and perpendicular (c, d) to the PbI_4^{2-} inorganic layers. Excess organic spacer cations have been removed from (c) and (d) to show the structural distortions of the perovskite lattices. Crystallography data for $(F\text{-PMA})_2PbI_4$ were obtained from Reference (10). (e) Powder X-ray diffraction patterns of the spin-coated thin films of $(CF_3\text{-PMA})_2PbI_4$ (blue) and $(F\text{-PMA})_2PbI_4$ (red). (f) UV−vis absorption spectra (dotted curves) and photoluminescence spectra (solid curves) of $(CF_3\text{-PMA})_2PbI_4$ (blue) and $(F\text{-PMA})_2PbI_4$ (red) films.

https://dx.doi.org/10.1021/acs.jpclett.0c02909
J. Phys. Chem. Lett. 2020, 11, 10144−10149

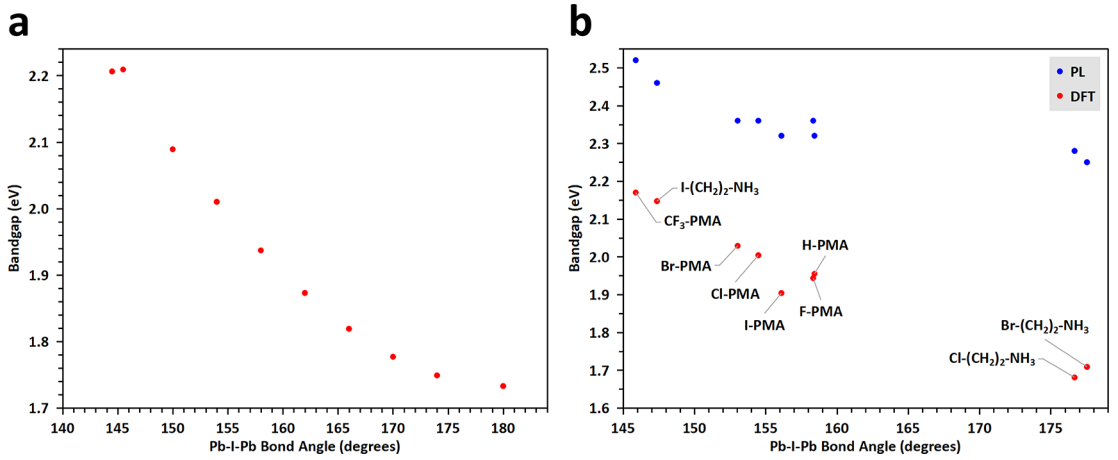

Figure 2. (a) Simulated results showing the negative relationship between the bandgap and Pb−I−Pb bond angle of a manually distorted negatively-charged inorganic 2D lead iodide perovskite layer without any ligands. (b) Comparison of experimentally-measured photoluminescence bandgap values (blue dots) of 2D lead iodide perovskites with those obtained by density functional theory calculations (red dots) based on single-crystal X-ray diffraction data.

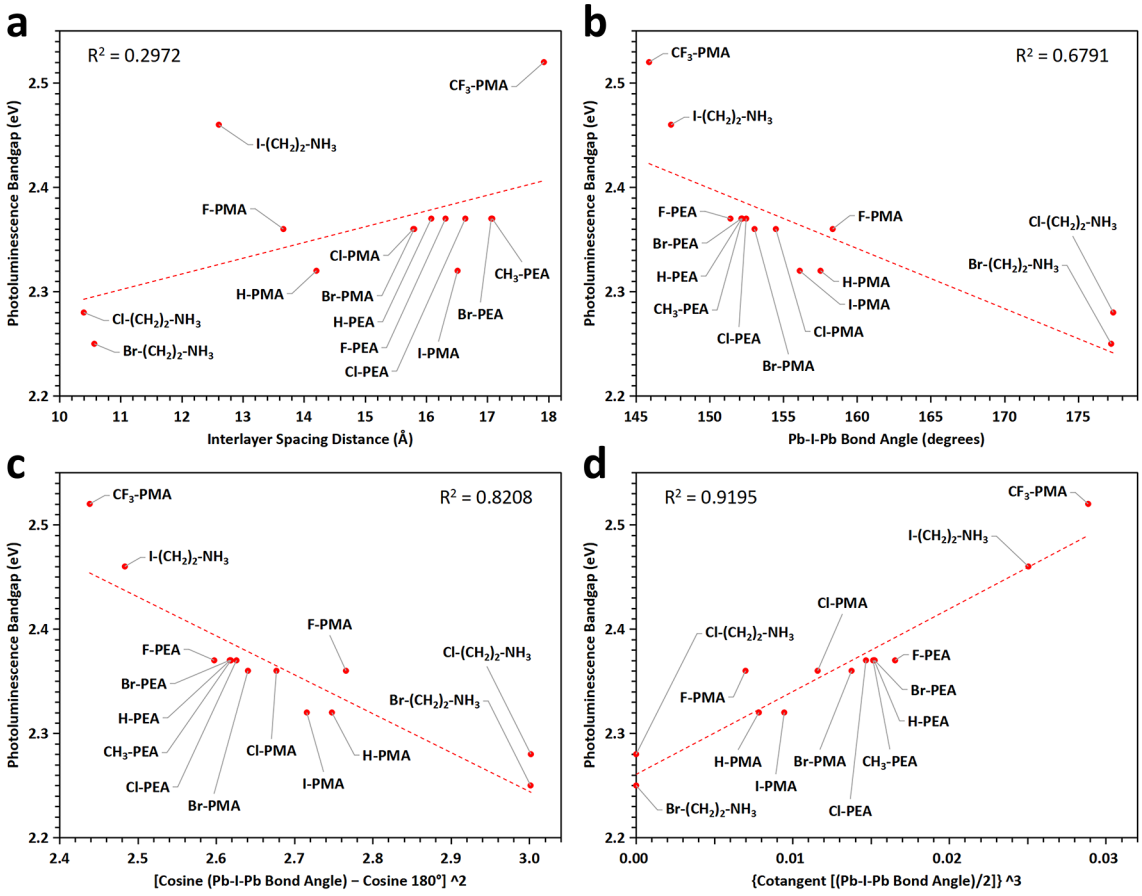

Figure 3. Relationships between the photoluminescence bandgap of 2D lead iodide perovskites and different structural parameters: the interlayer spacing distance (a), the average Pb−I−Pb bond angle (b), the cosine-harmonic bending potential (c), and the cubic value of the cotangent of half the Pb−I−Pb bond angle (d), which gives a more linear correlation compared with other relationships.

(trifluoromethyl)benzylamine (0.30 mol/L) was allowed to cool slowly to 298 K in a sealed glass vial without disturbance, giving bright yellow-colored plate-shaped crystals. The crystals were washed with toluene and dried thoroughly under vacuum at 298 K (Figure S1a). Thin films of $(CF_3\text{-PMA})_2PbI_4$ were prepared by spin-coating a solution of the crystals (with a lead concentration of 0.50 mol/L in a 1:1 volumetric mixture of *N*,*N*-dimethylformamide and dimethyl sulfoxide) onto oxygen-plasma-treated glass substrates at 4000 rpm for 30 seconds followed by annealing at 373 K for 10 min in air. As controls we used $(F\text{-PMA})_2PbI_4$, which was synthesized in a similar process by using 4-fluorobenzylamine as the organic precursor, giving orange-colored plate-shaped crystals (Figure S1b).

https://dx.doi.org/10.1021/acs.jpclett.0c02909
J. Phys. Chem. Lett. 2020, 11, 10144−10149

The crystal structure of $(CF_3\text{-PMA})_2PbI_4$ was investigated using single-crystal X-ray diffraction (XRD). This revealed periodically spaced inorganic sheets consisting of corner-sharing PbI_6 octahedra intercalated by layers of CF_3-PMA molecules. Unlike in the F-PMA perovskite, the trifluoromethyl group greatly reduces the overlap between oppositely-oriented CF_3-PMA spacers within each organic layer (Figure 1a,b and Figures S2 and S3).[10] This eliminates the possibility of $\pi-\pi$ stacking or π-halogen bonding between the aromatic moieties of benzylammonium cations and induces a greater structural distortion in the inorganic PbI_4^{2-} planes (quantitatively described as a smaller Pb−I−Pb bond angle) when compared with $(F\text{-PMA})_2PbI_4$ (Figure 1c,d and Table 1). Both films exhibited high crystallinity as evidenced by sharp peaks in the powder XRD spectra, and the strong periodicity of the peaks is characteristic of layered 2D perovskites (Figure 1e). We used ultraviolet−visible (UV−vis) absorption spectroscopy and photoluminescence spectroscopy to determine the bandgap of the films and found that the bandgap of the trifluoromethyl perovskite material is significantly blue-shifted compared to the fluoride control (Figure 1f).

To understand better the bandgap increase for the trifluoromethyl substitution, and to evaluate the contribution of structural distortion to the blue shift versus other changes from different organic spacer cations, we used density functional theory (DFT) to investigate the influence of the Pb−I−Pb bond angle on the highest occupied molecular orbital (HOMO) and lowest unoccupied molecular orbital (LUMO) energy levels of 2D lead iodide perovskites. When we manually distorted a single perovskite layer consisting of corner-sharing PbI_6 octahedra, we saw a nonlinear negative correlation between the bandgap and the Pb−I−Pb bond angle (Figure 2a), which is in agreement with the experimental results of Y-PMA, Y-PEA, and also β-substituted ethylamines (Figure 2b). These results indicate that the blue shift of $(CF_3\text{-PMA})_2PbI_4$ might be caused by the structural distortion of inorganic perovskite layers.

The positive relationship between structural distortion and bandgap in 2D perovskites has previously been posited.[9] We attempted to make the quantitative link between the crystal structure and bandgap of 2D lead iodide perovskites, plotting PL bandgap against different structural parameters. This includes the interlayer spacing distance (Figure 3a) and the Pb−I−Pb bond angle (Figure 3b). In addition, we used trigonometric functions including the square of the difference between cosine of the Pb−I−Pb bond angle and cosine 180°. This is part of the cosine- harmonic bond-angle potential energy function,[20,21] where the undistorted angle of 180° is used as the reference angle (Figure 3c). The final function we used was the cubic value of the cotangent of half the Pb−I−Pb bond angle (Figure 3d), where the trigonometric function transforms an angular value into a ratio of two lengths that could be directly associated with the distances between metal and halogen atoms. On the basis of the coefficient of determination (R-squared), a linear correlation between the photoluminescence bandgap and $(D/L)^3$ is plausible. Here, D is the distance from the midpoint of two lead atoms to the iodine atom that bridges them, and L is half the distance between the two lead atoms (Figure 3d). This correlation suggests that, in an idealized situation where other distortion effects such as the overlap between nearby iodides are ignored, a PL emission wavelength of 480 nm (2.58 eV) may be achieved if the Pb−I−Pb angle can be decreased to below 142°. We also evaluated the relationship between PL bandgap and other structural parameters such as the average intralayer Pb−Pb distance (Figure S4a) or its squared value (Figure S4b), as well as the average I−Pb−I bond angle (Table S1 and Figure S4c) and the average Pb−I bond length (Table S1 and Figure S 4d), but no linear correlation was observed.

In conclusion, we have synthesized a new type of 2D lead iodide perovskite with the formula $(CF_3\text{-PMA})_2PbI_4$, which exhibits significantly blue-shifted photoluminescence compared to both its halogen-substituted analogues $(Y\text{-PMA})_2PbI_4$ and a series of other 2D perovskites containing aromatic or aliphatic spacer cations. After comparing different structural parameters of these compounds, we confirmed that this increase in bandgap was a result of the distortion of the inorganic perovskite layers, which was in turn induced by the repulsive intermolecular interactions associated with the trifluoromethyl functional groups. We used DFT studies to account for this phenomenon and also saw a linear correlation between the bandgap and structural parameters to help estimate the extent of distortion required for deep-blue or violet photoluminescence. The behavior of organic spacers with perfluorinated substituents suggest an approach to developing perovskite-based blue light-emitting materials for application in laser or display technologies.

EXPERIMENTAL METHODS

Materials. Lead(II) iodide (99%, Sigma-Aldrich), 4-(trifluoromethyl)benzylamine (98%, TCI America), 4-fluorobenzylamine (97%, Sigma-Aldrich), hydriodic acid (57 wt % in H_2O, 99.95%, Sigma- Aldrich), hypophosphorous acid solution (50 wt % in H_2O, Sigma-Aldrich), toluene (99.5%, Fisher Chemical), *N*,*N*-dimethylformamide (anhydrous, 99.8%, Sigma-Aldrich), and dimethyl sulfoxide (anhydrous, 99.9%, Sigma-Aldrich) were used as received.

Synthesis. In a typical procedure, lead(II) iodide (415 mg) and 4-(trifluoromethyl)benzylamine (320 mg, about 260 uL) were completely dissolved in a mixed solution of hydriodic acid (5 mL, 57 wt % in water) and hypophosphorous acid (1 mL, 50 wt % in water) by heating at 373 K. Afterward, the system was allowed to cool to 298 K at a rate of 0.1 K/min to give yellow-colored $(CF_3\text{-PMA})_2PbI_4$ perovskite crystals. These crystals were collected by vacuum filtration, washed with toluene, and dried under vacuum at 298 K.

Following the same procedure as described above, two-dimensional perovskite crystals of $(F\text{-PMA})_2PbI_4$ could be synthesized by using 4-fluorobenzylamine (230 mg, about 210 μL) as the precursor of organic spacer cations.

Characterization. Powder XRD patterns were collected on a Rigaku MiniFlex 600 6G Benchtop powder X-ray diffraction instrument using Cu Kα radiation (λ = 1.5406 Å). UV−vis absorption spectroscopy was performed on a PerkinElmer LAMBDA 950 UV/vis/NIR spectrophotometer. Photoluminescence spectroscopy was conducted on a Horiba Fluorolog Time Correlated Single Photon Counting system equipped with UV/vis/NIR photomultiplier tube detectors. Single-crystal X-ray diffraction analysis was obtained on a Bruker Kappa APEX-DUO CCD Diffractometer using Mo Kα radiation (λ = 0.71073 Å).

ASSOCIATED CONTENT

Supporting Information

The Supporting Information is available free of charge at https://pubs.acs.org/doi/10.1021/acs.jpclett.0c02909.

https://dx.doi.org/10.1021/acs.jpclett.0c02909
J. Phys. Chem. Lett. 2020, 11, 10144−10149

Photographs of crystals, crystal structures, selected structural and optical properties, and photoluminescence bandgap vs distances and angles (PDF)

Crystallographic data for $(CF_3\text{-PMA})_2PbI_4$ (CIF)

AUTHOR INFORMATION

Corresponding Author

Edward H. Sargent − *Department of Electrical and Computer Engineering, University of Toronto, Toronto, Ontario M5S 3G4, Canada;* orcid.org/0000-0003-0396-6495; Email: ted.sargent@utoronto.ca

Authors

Pei-Xi Wang − *Department of Electrical and Computer Engineering, University of Toronto, Toronto, Ontario M5S 3G4, Canada;* orcid.org/0000-0003-0683-4818

Amin Morteza Najarian − *Department of Electrical and Computer Engineering, University of Toronto, Toronto, Ontario M5S 3G4, Canada;* orcid.org/0000-0002-0455-0451

Zhaomin Hao − *Department of Physical and Environmental Sciences, University of Toronto Scarborough, Scarborough, Ontario M1C 1A4, Canada*

Andrew Johnston − *Department of Electrical and Computer Engineering, University of Toronto, Toronto, Ontario M5S 3G4, Canada;* orcid.org/0000-0002-4545-532X

Oleksandr Voznyy − *Department of Physical and Environmental Sciences, University of Toronto Scarborough, Scarborough, Ontario M1C 1A4, Canada;* orcid.org/0000-0002-8656-5074

Sjoerd Hoogland − *Department of Electrical and Computer Engineering, University of Toronto, Toronto, Ontario M5S 3G4, Canada;* orcid.org/0000-0002-3099-585X

Complete contact information is available at: https://pubs.acs.org/10.1021/acs.jpclett.0c02909

Notes

The authors declare no competing financial interest.

ACKNOWLEDGMENTS

This work was financially supported by Huawei Technologies Canada Co., Ltd., and Natural Sciences and Engineering Research Council of Canada (NSERC). The authors acknowledge Dr. Alan J. Lough for his assistance with X-ray crystallography. Computations were performed on the Niagara supercomputer at the SciNet HPC Consortium. SciNet is funded by the Canada Foundation for Innovation, the Government of Ontario, Ontario Research Fund - Research Excellence, and the University of Toronto.

REFERENCES

(1) Dieter, W. CH3NH3PbX3, ein Pb(II)-System mit kubischer Perowskitstruktur / CH3NH3PbX3, a Pb(II)-System with Cubic Perovskite Structure. *Z. Naturforsch., B: J. Chem. Sci.* **1978**, *33*, 1443−1445.

(2) Stranks, S. D.; Snaith, H. J. Metal-halide perovskites for photovoltaic and light-emitting devices. *Nat. Nanotechnol.* **2015**, *10*, 391−402.

(3) Zhang, F.; Lu, H.; Tong, J.; Berry, J. J.; Beard, M. C.; Zhu, K. Advances in two-dimensional organic-inorganic hybrid perovskites. *Energy Environ. Sci.* **2020**, *13*, 1154−1186.

(4) Mitzi, D. B. Synthesis, Crystal Structure, and Optical and Thermal Properties of (C4H9NH3)2MI4 (M = Ge, Sn, Pb). *Chem. Mater.* **1996**, *8*, 791−800.

(5) Mitzi, D. B.; Dimitrakopoulos, C. D.; Kosbar, L. L. Structurally Tailored Organic-Inorganic Perovskites: Optical Properties and Solution-Processed Channel Materials for Thin-Film Transistors. *Chem. Mater.* **2001**, *13*, 3728−3740.

(6) Xu, Z.; Mitzi, D. B. SnI42–Based Hybrid Perovskites Templated by Multiple Organic Cations: Combining Organic Functionalities through Noncovalent Interactions. *Chem. Mater.* **2003**, *15*, 3632−3637.

(7) Xu, Z.; Mitzi, D. B.; Dimitrakopoulos, C. D.; Maxcy, K. R. Semiconducting Perovskites (2- XC6H4C2H4NH3)2SnI4 (X = F, Cl, Br): Steric Interaction between the Organic and Inorganic Layers. *Inorg. Chem.* **2003**, *42*, 2031−2039.

(8) Xu, Z.; Mitzi, D. B.; Medeiros, D. R. [(CH3)3NCH2CH2NH3]-SnI4: A Layered Perovskite with Quaternary/Primary Ammonium Dications and Short Interlayer Iodine-Iodine Contacts. *Inorg. Chem.* **2003**, *42*, 1400−1402.

(9) Knutson, J. L.; Martin, J. D.; Mitzi, D. B. Tuning the Band Gap in Hybrid Tin Iodide Perovskite Semiconductors Using Structural Templating. *Inorg. Chem.* **2005**, *44*, 4699−4705.

(10) Tremblay, M.-H.; Bacsa, J.; Zhao, B.; Pulvirenti, F.; Barlow, S.; Marder, S. R. Structures of (4-Y-C6H4CH2NH3)2PbI4 {Y = H, F, Cl, Br, I}: Tuning of Hybrid Organic Inorganic Perovskite Structures from Ruddlesden-Popper to Dion-Jacobson Limits. *Chem. Mater.* **2019**, *31*, 6145−6153.

(11) Du, K.-z.; Tu, Q.; Zhang, X.; Han, Q.; Liu, J.; Zauscher, S.; Mitzi, D. B. Two-Dimensional Lead(II) Halide-Based Hybrid Perovskites Templated by Acene Alkylamines: Crystal Structures, Optical Properties, and Piezoelectricity. *Inorg. Chem.* **2017**, *56*, 9291−9302.

(12) Straus, D. B.; Iotov, N.; Gau, M. R.; Zhao, Q.; Carroll, P. J.; Kagan, C. R. Longer Cations Increase Energetic Disorder in Excitonic 2D Hybrid Perovskites. *J. Phys. Chem. Lett.* **2019**, *10*, 1198−1205.

(13) Sourisseau, S.; Louvain, N.; Bi, W.; Mercier, N.; Rondeau, D.; Boucher, F.; Buzaré, J.-Y.; Legein, C. Reduced Band Gap Hybrid Perovskites Resulting from Combined Hydrogen and Halogen Bonding at the Organic-Inorganic Interface. *Chem. Mater.* **2007**, *19*, 600−607.

(14) Schmitt, T.; Bourelle, S.; Tye, N.; Soavi, G.; Bond, A. D.; Feldmann, S.; Traore, B.; Katan, C.; Even, J.; Dutton, S. E.; Deschler, F. Control of Crystal Symmetry Breaking with Halogen- Substituted Benzylammonium in Layered Hybrid Metal-Halide Perovskites. *J. Am. Chem. Soc.* **2020**, *142*, 5060−5067.

(15) Mantsyzov, A. B.; Sokolov, M. N.; Ivantcova, P. M.; Bräse, S.; Polshakov, V. I.; Kudryavtsev, K. V. Interplay of Pyrrolidine Units with Homo/Hetero Chirality and CF3-Aryl Substituents on Secondary Structures of β-Proline Tripeptides in Solution. *J. Org. Chem.* **2020**, *85*, 8865.

(16) Nagai, T.; Nishioka, G.; Koyama, M.; Ando, A.; Miki, T.; Kumadaki, I. Reactions of trifluoromethyl ketones. IX. Investigation of the steric effect of a trifluoromethyl group based on the stereochemistry on the dehydration of trifluoromethyl homoallyl alcohols. *J. Fluorine Chem.* **1992**, *57*, 229−237.

(17) Suzuki, M.; Okada, T.; Taguchi, T.; Hanzawa, Y.; Iitaka, Y. Intramolecular Diels-Alder reactions of furan derivatives: Steric and electronic effects of trifluoromethyl groups. *J. Fluorine Chem.* **1992**, *57*, 239−243.

(18) Corbett, M. S.; Liu, X.; Sanyal, A.; Snyder, J. K. Cycloadditions of chiral anthracenes: effect of the trifluoromethyl group. *Tetrahedron Lett.* **2003**, *44*, 931−935.

(19) Katagiri, T.; Uneyama, K. Stereospecific substitution at α-carbon to trifluoromethyl group: Application to optically active fluorinated amino acid syntheses. *Chirality* **2003**, *15*, 4−9.

(20) Balasundaram, R.; Jiang, S.; Belak, J. Structural and rheological properties of n-decane confined between graphite surfaces. *Chem. Eng. J.* **1999**, *74*, 117−127.

(21) Zhang, L.; Balasundaram, R.; Gehrke, S. H.; Jiang, S. Nonequilibrium molecular dynamics simulations of confined fluids in contact with the bulk. *J. Chem. Phys.* **2001**, *114*, 6869−6877.

https://dx.doi.org/10.1021/acs.jpclett.0c02909
J. Phys. Chem. Lett. 2020, 11, 10144−10149